A Modular Nonlinear Continuous-Discrete Filter for Concurrent 3D Robot Pose and Landmark Position Estimation

Behzad Zamani[1] and Jochen Trumpf[2]

***Abstract*— This paper proposes a modular nonlinear minimum energy filtering approach for concurrent estimation of the 3D pose of a mobile robot in the Special Euclidean Group $\mathrm{SE}(3)$ and the unknown 3D position of a stationary landmark for the common situation where relative position measurements to the landmark are obtained in discrete time and are too infrequent or too irregular to allow modeling of the measurement process in continuous time. Building on previous work by the authors that treated the case of 3D robot pose estimation on $\mathrm{SE}(3)$ with known 3D landmark positions using the Geometric Approximate Minimum Energy (GAME) filtering framework, we show how to incorporate an additional nonlinear filter for concurrent estimation of the unknown 3D position of a stationary landmark. The proposed approach is fully modular in the sense that either filter could be swapped out for an alternative design without impacting the functionality of the remaining filter. In particular, the approach does not require tracking of error cross-covariance information between both filters and instead uses a nonlinear version of Covariance Intersection (CI) to perform safe information fusion at each filter node. We demonstrate the performance of the proposed modular filter in a numerical simulation showing that it achieves comparable results to the filter that requires all landmark positions to be known.**

I. INTRODUCTION

With increasing complexity of modern robotic applications, modular designs for filters that estimate the system state are of increasing interest. Simultaneous Localization and Mapping (SLAM) [1], [2], target tracking [3], collaborative localization [4], self-driving cars [5], and augmented/virtual reality headsets [6] are examples of robotic applications where multiple separate subsystems receive and process measurement data and contribute to the decision making in the overall system. In a monolithic filter design, the subsystem states are concatenated into a joint system state and a single filtering algorithm updates the full state estimate based on all measurement data. In practice, the development of complex systems proceeds iteratively and benefits from modular approaches to the measurement and fusion of sensor data. Modularity helps to manage storage and computational complexity of filtering algorithms by avoiding large state vector representations and error covariance matrices, it helps to separate concerns in the sense that a software bug or bad performance in one filtering module does not immediately affect other modules, it simplifies debugging and change management and improves interoperability.

[1]Behzad Zamani is with the Department of Electrical and Electronics Engineering, The University of Melbourne, Australia, email: behzad.zamani@unimelb.edu.au. [2]Jochen Trumpf is with the School of Engineering, Australian National University, Australia. email: jochen.trumpf@anu.edu.au.

In this paper we build on previous work by the authors [7] that treated the case of 3D robot pose estimation on $\mathrm{SE}(3)$ given interoceptive velocity measurements and relative position measurements to known 3D landmark positions using the nonlinear Geometric Approximate Minimum Energy (GAME) filtering framework [8]. The filter proposed in [7] is a continuous-discrete version of the GAME filter in which high frequency and regular interoceptive measurements are applied in a continuous-time design for the propagation step, while exteroceptive measurements which may arrive irregularly or infrequently are incorporated through a discrete-time update step. We show how to augment this design with an additional filter for concurrent estimation of the unknown 3D position of a stationary landmark while at the same time using the relative measurement to the position of that landmark as one of the inputs to the robot pose filter. In this situation, information exchanged between both filters is not statistically independent and does not contain tracked cross correlations [9], [10] to enable a fully modular design. To avoid double counting of information we provide a nonlinear version of the Covariance Intersection (CI) algorithm [11] based on least squares filtering techniques to safely fuse estimates with unknown correlation caused by loops in the information flow graph that describes how the two subsystems exchange information. We demonstrate the performance of the proposed modular filter in a numerical simulation.

The remainder of the paper is organized as follows. Section II introduces our notation and recalls the standard matrix representation of the Special Euclidean group $\mathrm{SE}(3)$ and its matrix calculus as well as related relevant notions from differential geometry. Section III introduces the modular concurrent 3D robot pose and 3D landmark position estimation problem. Section IV contains our main result, the proposed modular GAME filter for this problem. In Section V we demonstrate the performance of the proposed filter in a numerical simulation and Section VI concludes the paper.

II. PRELIMINARIES

Let $\mathcal{A}$ denote the global reference frame and let $\mathcal{B}$ denote a frame fixed to a moving rigid body in 3D space. The translation of $\mathcal{B}$ with respect to $\mathcal{A}$, expressed in $\mathcal{A}$, is denoted as $p \in \mathbb{R}^3$. The attitude (orientation) of $\mathcal{B}$ relative to the reference frame $\mathcal{A}$, expressed in $\mathcal{A}$, is represented by a rotation matrix $R \in \mathrm{SO}(3) = \{R \in \mathbb{R}^{3\times 3} \,|\, R^\top R = I, \det(R) = 1\}$, where $(.)^\top$ is the transpose map, I is the 3 by 3 identity matrix and $\det(.)$ is the matrix determinant. The Lie algebra $\mathfrak{so}(3)$ associated with the matrix Lie group

979-8-3315-2649-8/25/$31.00 ©2025 IEEE

$\mathrm{SO}(3)$ is the set of skew-symmetric matrices, $\mathfrak{so}(3) = \{\omega_\times \in \mathbb{R}^{3\times 3} \,|\, \omega_\times = -\omega_\times^\top\}$. For $\omega = [\omega_1, \omega_2, \omega_3]^\top \in \mathbb{R}^3$, the lower index operator $(.)_\times \colon \mathbb{R}^3 \longrightarrow \mathfrak{so}(3)$ yields the skew-symmetric matrix

$$\omega_\times \coloneqq \begin{bmatrix} 0 & -\omega_3 & \omega_2 \\ \omega_3 & 0 & -\omega_1 \\ -\omega_2 & \omega_1 & 0 \end{bmatrix}.$$

This skew-symmetric matrix is associated with the cross product by ω, i.e. $\omega_\times v = \omega \times v$ for all $v \in \mathbb{R}^3$. Inversely, the operator **vex**: $\mathfrak{so}(3) \longrightarrow \mathbb{R}^3$ extracts the skew coordinates, $\mathbf{vex}(\omega_\times) \coloneqq \omega$.

A pose matrix consisting of attitude R and translation p of the body fixed frame $\mathcal{B}$ with respect to the global reference frame $\mathcal{A}$ can be represented as $X = \begin{bmatrix} R & p \\ 0_{1\times 3} & 1 \end{bmatrix} \in \mathrm{SE}(3)$ where

$$\mathrm{SE}(3) = \left\{ \begin{bmatrix} R & p \\ 0_{1\times 3} & 1 \end{bmatrix} \in \mathbb{R}^{4\times 4} \;\middle|\; R \in \mathrm{SO}(3),\ p \in \mathbb{R}^3 \right\}$$

denotes the Special Euclidean group represented in homogeneous coordinates. The inverse pose X^{-1} is given by

$$X^{-1} = \begin{bmatrix} R^\top & -R^\top p \\ 0_{1\times 3} & 1 \end{bmatrix}.$$

The Lie algebra associated with the matrix Lie group $\mathrm{SE}(3)$ is the set of twist matrices

$$\mathfrak{se}(3) = \left\{ \Gamma \coloneqq \begin{bmatrix} (\Gamma_\omega)_\times & \Gamma_v \\ 0_{1\times 3} & 0 \end{bmatrix} \in \mathbb{R}^{4\times 4} \mid \Gamma_\omega, \Gamma_v \in \mathbb{R}^3 \right\}.$$

The map $(.)^\wedge \colon \mathbb{R}^6 \longrightarrow \mathfrak{se}(3)$ and its inverse $(.)^\vee \colon \mathfrak{se}(3) \longrightarrow \mathbb{R}^6$ are defined as

$$\begin{bmatrix} \Gamma_\omega \\ \Gamma_v \end{bmatrix}^\wedge \coloneqq \begin{bmatrix} (\Gamma_\omega)_\times & \Gamma_v \\ 0_{1\times 3} & 0 \end{bmatrix}, \quad \left(\begin{bmatrix} \Gamma_\omega \\ \Gamma_v \end{bmatrix}^\wedge \right)^\vee \coloneqq \begin{bmatrix} \Gamma_\omega \\ \Gamma_v \end{bmatrix}. \tag{1}$$

For two $\mathrm{SE}(3)$ elements X_1, X_2 such that $X_2^{-1}X_1 \in \mathcal{D}_{\mathbf{log}}$ and a positive definite matrix $P \in \mathbb{R}^{6\times 6} > 0$, the weighted Euclidean distance is defined as

$$\|X_1 - X_2\|_{P^{-1}} \coloneqq \sqrt{\langle (P^{-1}\,\mathbf{log}(X_2^{-1}X_1)^\vee)^\wedge, \mathbf{log}(X_2^{-1}X_1)\rangle}. \tag{2}$$

Here, $\mathbf{log}(.) \colon \mathcal{D}_{\mathbf{log}} \subset \mathrm{SE}(3) \longrightarrow \mathfrak{se}(3)$ is the matrix logarithm defined on the maximal domain $\mathcal{D}_{\mathbf{log}}$ such that $I \in \mathcal{D}_{\mathbf{log}} \subset \mathrm{SE}(3)$.

Given any matrix $M \in \mathbb{R}^{n\times n}$, its symmetric and skew-symmetric projections are defined as $\mathbb{P}_s(M) \coloneqq 1/2(M + M^\top)$ and $\mathbb{P}_a(M) \coloneqq 1/2(M - M^\top)$, respectively. Note that for all $\Omega_\times \in \mathfrak{so}(3)$, $M \in \mathbb{R}^{3\times 3}$ and $S = S^\top \in \mathbb{R}^{3\times 3}$,

$$\mathbf{trace}(\Omega_\times \mathbb{P}_s(M)) = 0,\ \mathbf{trace}(\mathbb{P}_s(S\Omega_\times)) = 0. \tag{3}$$

Here, $\mathbf{trace}(.) \colon \mathbb{R}^{n\times n} \longrightarrow \mathbb{R}$ is the matrix trace function.

We will draw on the following identities in the paper. Let $\gamma, \psi \in \mathbb{R}^3$, then

$$\begin{aligned} &\gamma_\times \psi_\times = \psi\gamma^\top - \gamma^\top \psi I, \\ &\mathbb{P}_a(\gamma_\times \psi_\times) = \mathbb{P}_a(\psi\gamma^\top) = \frac{1}{2}(\gamma \times \psi)_\times = \frac{1}{2}(\gamma_\times \psi)_\times. \end{aligned} \tag{4}$$

A. Differential Geometric Notions

Let $T_X\,\mathrm{SE}(3)$ denote the tangent space to the manifold $\mathrm{SE}(3)$ at X. Note that the Lie algebra $\mathfrak{se}(3)$ is identified with $T_I\,\mathrm{SE}(3)$. For all $\Gamma \in \mathfrak{se}(3)$ then $X\Gamma \in T_X\,\mathrm{SE}(3)$. Let $\langle .,. \rangle \colon T\,\mathrm{SE}(3) \times T\,\mathrm{SE}(3) \longrightarrow \mathbb{R}$ denote the standard left-invariant Riemannian metric on $\mathrm{SE}(3)$, i.e.

$$\langle X\Gamma, X\Omega \rangle_X = \langle \Gamma, \Omega \rangle_I = \mathbf{trace}(\frac{\mathbf{1}}{\mathbf{2}}\Gamma^\top \Omega) = (\Gamma^\vee)^\top \Omega^\vee. \tag{5}$$

Here,

$$\frac{\mathbf{1}}{\mathbf{2}} \coloneqq \begin{bmatrix} \frac{1}{2}I_{3\times 3} & 0_{3\times 1} \\ 0_{1\times 3} & 1 \end{bmatrix} \quad \text{and} \quad \mathbf{2} \coloneqq \begin{bmatrix} 2I_{3\times 3} & 0_{3\times 1} \\ 0_{1\times 3} & 1 \end{bmatrix}.$$

Let $\mathbb{P} \colon \mathbb{R}^{4\times 4} \to \mathfrak{se}(3)$ denote the unique orthogonal projection of $\mathbb{R}^{4\times 4}$ onto $\mathfrak{se}(3)$ with respect to the inner product

$$\langle A, B \rangle_{\frac{\mathbf{1}}{\mathbf{2}}} = \mathbf{trace}(\frac{\mathbf{1}}{\mathbf{2}} A^\top B),$$

i.e. for all $\Gamma \in \mathfrak{se}(3)$, $M \in \mathbb{R}^{4\times 4}$, one has

$$\langle \Gamma, M \rangle_{\frac{\mathbf{1}}{\mathbf{2}}} = \langle \Gamma, \mathbb{P}(M) \rangle_{\frac{\mathbf{1}}{\mathbf{2}}} = \langle \mathbb{P}(M), \Gamma \rangle_{\frac{\mathbf{1}}{\mathbf{2}}}.$$

One verifies that for all $M_1 \in \mathbb{R}^{3\times 3}, m_{2,3} \in \mathbb{R}^3, m_4 \in \mathbb{R}$,

$$\mathbb{P}\left(\begin{bmatrix} M_1 & m_2 \\ m_3^\top & m_4 \end{bmatrix} \right) = \begin{bmatrix} \mathbb{P}_a(M_1) & m_2 \\ 0_{1\times 3} & 0 \end{bmatrix}.$$

Let $f \colon \mathrm{SE}(3) \longrightarrow \mathbb{R}$ denote a differentiable map. Then $\mathcal{D}_X f(X) \colon T_X\,\mathrm{SE}(3) \longrightarrow \mathbb{R}$ denotes the differential of f at the point $X \in \mathrm{SE}(3)$. We have

$$\mathcal{D}_X f(X) \circ (X\Gamma) = \langle \nabla_X f(X), X\Gamma \rangle_X \tag{6}$$

for all $\Gamma \in \mathfrak{se}(3)$ where $\nabla_X f(X) \in T_X\,\mathrm{SE}(3)$ is the gradient of f at the point $X \in \mathrm{SE}(3)$. Similarly, the second order differential $\mathcal{D}_X^2 f(X) \colon T_X\,\mathrm{SE}(3) \times T_X\,\mathrm{SE}(3) \longrightarrow \mathbb{R}$ fulfils

$$\begin{aligned} &\mathcal{D}_X^2 f(X) \circ (X\Gamma, X\Xi) = \langle \mathbf{Hess}_X\, f(X) \circ X\Psi, X\Gamma \rangle_X \\ &= \langle \mathbf{Hess}_X\, f(X) \circ X\Gamma, X\Psi \rangle_X \end{aligned} \tag{7}$$

for all $\Gamma, \Psi \in \mathfrak{se}(3)$ where the Hessian $\mathbf{Hess}_X\, f(X) \colon T_X\,\mathrm{SE}(3) \longrightarrow T_X\,\mathrm{SE}(3)$ is a symmetric mapping with respect to the left invariant metric. In another form,

$$\begin{aligned} &\mathcal{D}_X^2 f(X) \circ (X\Gamma, X\Psi) = \\ &D_X(\mathcal{D}_X f(X) \circ (X\Gamma)) \circ X\Psi - \langle \nabla_X f(X), X\,\mathbf{\Lambda}_\Psi(\Gamma) \rangle_X. \end{aligned}$$

Here, $\mathbf{\Lambda}_\Psi(.) \colon \mathfrak{se}(3) \longrightarrow \mathfrak{se}(3)$ is the connection function. In this paper we will use the symmetric Cartan-Schouten 0-connection on $\mathrm{SE}(3)$ given by

$$\mathbf{\Lambda}_\Psi(\Gamma) \coloneqq \frac{1}{2}[\Psi, \Gamma] = \frac{1}{2}(\Psi\Gamma - \Gamma\Psi) \tag{8}$$

for all $\Gamma, \Psi \in \mathfrak{se}(3)$. Here, $[.,.] \colon \mathfrak{se}(3) \times \mathfrak{se}(3) \longrightarrow \mathfrak{se}(3)$ is the Lie bracket of $\mathfrak{se}(3)$. One verifies that

$$(\mathbf{\Lambda}_\Psi(\Gamma))^\vee = \frac{1}{2}\begin{bmatrix} \Psi_\omega \times \Gamma_\omega \\ \Psi_\omega \times \Gamma_v - \Gamma_\omega \times \Psi_v \end{bmatrix}. \tag{9}$$

III. Problem Formulation

In this section we state the left invariant kinematics on $\mathrm{SE}(3)$, introduce models for interoceptive and exteroceptive measurements and formalize the filtering problem using these models.

A. Pose Kinematics

Let $X = \begin{bmatrix} R & p \\ 0_{1\times 3} & 1 \end{bmatrix}$ denote the pose matrix of a moving body in 3D space. The left invariant pose kinematics on $\mathrm{SE}(3)$ is given by

$$\dot{X} = X \begin{bmatrix} \Omega \\ V \end{bmatrix}^{\wedge}, \; X(0) = X_0. \tag{10}$$

Recall that $R \in \mathrm{SO}(3)$ is the attitude and $p \in \mathbb{R}^3$ the translation of the body fixed frame $\mathcal{B}$ with respect to the global reference frame $\mathcal{A}$. The matrix $\begin{bmatrix} \Omega \\ V \end{bmatrix}^{\wedge} \in \mathfrak{se}(3)$ is the twist and embodies the angular velocity $\Omega \in \mathbb{R}^3$ and translational velocity $V \in \mathbb{R}^3$ of the body fixed frame $\mathcal{B}$ with respect to the global reference frame $\mathcal{A}$, expressed in $\mathcal{B}$.

B. Velocity Measurements

The measured twist is comprised of angular and translational velocity measured in the body fixed frame $\mathcal{B}$ as represented by the following equations

$$\begin{aligned} &U \coloneqq \begin{bmatrix} \Omega \\ V \end{bmatrix}^{\wedge} + (B\delta)^{\wedge}, \; B \coloneqq \begin{bmatrix} B_\omega & 0_{3\times 3} \\ 0_{3\times 3} & B_v \end{bmatrix}, \; \delta \coloneqq \begin{bmatrix} \delta_\omega \\ \delta_v \end{bmatrix}, \\ &U_\omega = \Omega + B_\omega \delta_\omega, \; U_v = V + B_v \delta_v, \end{aligned} \tag{11}$$

where $B_\omega, B_v \in \mathbb{R}^{3\times 3}$ are measurement error coefficient matrices determined from the sensor properties while $\delta_\omega, \delta_v \in \mathbb{R}^3$ are the unknown (here assumed zero mean) angular and translational velocity measurement errors.

C. Landmark Measurements

One can indirectly obtain further information on the pose of a moving body by measuring the relative position of an identifiable (e.g. via visually unique characteristics) landmark with respect to the body fixed frame,

$$\bar{y} = X^{-1}\bar{l} + \tilde{D}\mathring{\epsilon}. \tag{12}$$

Here the mappings $\bar{(.)}, \mathring{(.)} \colon \mathbb{R}^3 \longrightarrow \mathbb{R}^4$ and $\tilde{(.)} \colon \mathbb{R}^{3\times 3} \longrightarrow \mathbb{R}^{4\times 4}$ are defined as $\bar{x} \coloneqq [x, 1]^\top$ and $\mathring{x} \coloneqq [x, 0]^\top$ and $\tilde{D} \coloneqq \begin{bmatrix} D & 0_{3\times 1} \\ 0_{1\times 3} & 1 \end{bmatrix}$, respectively. The vector $y \in \mathbb{R}^3$ is the measured landmark position in $\mathcal{B}$, $l \in \mathbb{R}^3$ is the position of the landmark in the global reference frame $\mathcal{A}$, $\epsilon \in \mathbb{R}^3$ is the measurement error incurred in $\mathcal{B}$ where $D \in \mathbb{R}^{3\times 3}$ is the measurement error coefficient matrix determined based on the sensor properties.

Equation (12) is alternatively expressed as

$$y = R^\top (l - p) + D\epsilon. \tag{13}$$

Note that well-posedness of the full six degree of freedom pose filtering problem typically relies on at least three non-collinear fixed landmark measurements [12].

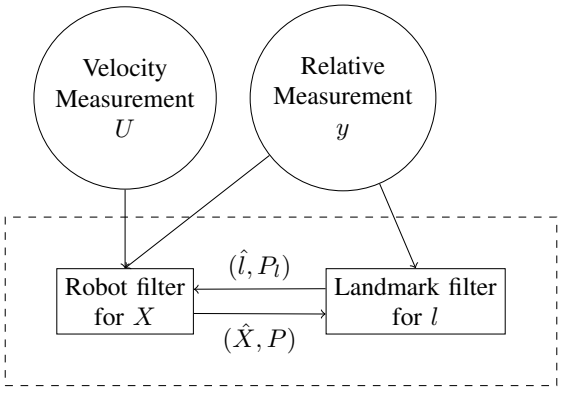

Fig. 1. Modular Filter Architecture

D. Modular Robot Pose and Landmark Position Estimation

We wish to recursively estimate the robot pose X based on the available velocity and landmark measurements using a nonlinear filtering algorithm to produce an estimate $\hat{X}$. In the case where a landmark position l is unknown in the global reference frame $\mathcal{A}$ (think for example of a visually distinctive feature in the environment that has not been referenced to a global map), we wish to concurrently and recursively estimate l using an additional nonlinear filtering algorithm to produce an estimate $\hat{l}$. Both algorithms exchange their current estimates in every update step to enable incorporation of the relative landmark position measurement y by substituting $\hat{X}$ for the unknown X and $\hat{l}$ for the unknown l. Figure 1 depicts the information flow between the two algorithm modules.

IV. Filter design

In this section we provide two algorithms, one for recursive estimation of the robot pose ($X \in \mathrm{SE}(3)$) and one for recursive estimation of the landmark position ($l \in \mathbb{R}^3$). The robot pose filter from our previous work [7] assumed that every landmark position is known in the global reference frame $\mathcal{A}$. Here, we will extend this filter to the case of an estimated landmark.

A. Robot Pose Prediction

First we provide the equations for the prediction step of the robot pose filter based on velocity measurements (11). Velocity measurements are often available with a reliable high update rate (compared to landmark measurements) and can be modeled as continuous-time signals.

Let us consider the continuous-time filtering cost

$$J_t(X, \delta) \coloneqq \frac{1}{2}\|X(0) - \hat{X}_0\|^2_{P_0^{-1}} + \frac{1}{2}\int_0^t \|\delta(\tau)\|^2 d\tau. \tag{14}$$

The first term in (14) is the initialization error between the true pose $X(0)$ and an a priori known estimate $\hat{X}_0 \in \mathrm{SE}(3)$ measured as a squared Euclidean distance (2) weighted with the positive definite error covariance matrix $P_0 \in \mathbb{R}^{6\times 6}$. The second integral term in (14) is the accumulated squared Euclidean norm of the velocity measurement error (11).

The cost (14) is minimized in two steps. The first step is to minimize (14) over the measurement error trajectory $\delta|_{[0,t]}$ and the second step is to minimize the result over the pose trajectory $X|_{[0,t]}$. The latter step can equivalently be simplified to minimizing over a single point of the pose trajectory, e.g. the start point $X(0)$, the end point $X(t)$ or any other point in between. Refer to [7], [8] for a more in-depth discussion of the rationale behind the minimum energy filtering approach.

The value of the first minimization step can be encoded using the value function

$$\begin{aligned} V(X,t) &\coloneqq \min_{\delta|_{[0,t]}} J_t(X,\delta), \\ V(X(0),0) &= \frac{1}{2}\|X(0)-\hat{X}_0\|^2_{P_0^{-1}}. \end{aligned} \tag{15}$$

Then

$$\hat{X}(t) \coloneqq \operatorname*{argmin}_X V(X,t)(t), \tag{16}$$

where X is any point of the true pose trajectory $X|_{[0,t]}$.

Interpreted differently, the value function (15) is an error energy or uncertainty measure for the true pose trajectory $X|_{[0,t]}$ at the time instance t. Accordingly, the estimate $\hat{X}(t)$ emerges as the minimizing point of this error energy measure and hence is called the minimum-energy estimate [13].

Robot Pose Prediction: The following prediction equations are from [7]. Note that the second equation in Equation (18) is written based on the error covariance P while in [7] this equation was written in terms of the inverse of the error covariance. Here, the error covariance corresponds to the inverse of the Hessian of the value function.

Definition 1 (Error Covariance Matrix): Given any two tangent directions $X\Gamma, X\Psi \in T_X\,\mathrm{SE}(3)$, the Hessian $\mathbf{Hess}_X\, V(X,t)|_{X=\hat{X}(t)}$ acting as a symmetric mapping as in (7) is equivalently represented with a positive definite matrix $P^{-1} \in \mathbb{R}^{6\times 6}$ operating on vectors $\Gamma^\vee, \Psi^\vee \in \mathbb{R}^6$ by

$$\langle P^{-1}\Psi^\vee, \Gamma^\vee\rangle \coloneqq \langle \mathbf{Hess}_X\, V(X,t)\circ X\Psi, X\Gamma\rangle_{X=\hat{X}(t)}. \tag{17}$$

The prediction step of the robot pose filter is then

$$\begin{aligned} \dot{\hat{X}}(t) &= \hat{X}(t)U(t),\ \hat{X}(0)=\hat{X}_0, \\ \dot{P}(t) &= BB^\top - 2\mathbb{P}_s\left(\begin{bmatrix}(U_\omega)_\times & 0_{3\times 3}\\ (U_v)_\times & (U_\omega)_\times\end{bmatrix} P\right). \end{aligned} \tag{18}$$

Note that we have added a factor of 2 for the symmetric projection term which was missing in [7, Eq. (35)].

Robot Pose Update: So far, we did not consider improving the estimated pose $\hat{X}(t)$ based on the landmark measurements (12). Assume that a landmark measurement $\bar{y}(t)$ becomes sporadically available at time t. We would like to update the current estimate $\hat{X}(t)$ to a new estimate $\hat{X}^+(t)$ based on this new information.

The landmark filter presented further below provides an estimate $(\hat{l}(t), P_l)$ of the landmark position and its error covariance. By minimizing the cost

$$\begin{aligned} J(X,l) =& \frac{1}{2}\|\bar{y}(t) - X^{-1}(t)\bar{l}\|^2_{(\tilde{D}\tilde{D}^\top)^{-1}} \\ &+ \frac{1}{2}\|l(t)-\hat{l}(t)\|^2_{P_l(t)^{-1}} \end{aligned} \tag{19}$$

with respect to l we can obtain a measurement purely dependent on the unknown $X(t)$. The optimal cost value in terms of X is then

$$J^*(X) = \frac{1}{2}\|\bar{y}(t) - X^{-1}(t)\bar{\hat{l}}\|^2_{\tilde{W}^{-1}}, \tag{20}$$

where $W \triangleq DD^\top + \hat{R}^\top P_l \hat{R}$.

When combining this cost with the value function from the prediction step of the filter, we need to account for the fact that these two pieces of information are now not statistically independent as the two filters shared information in previous filtering steps. This phenomenon is well known and has given rise to extensive research on safe fusion of correlated information in the absence of cross covariance information, see for example [11], [14]. The Covariance Intersection (CI) algorithm [11] provides the optimal safe solution to this problem [15]. Let $0 \le \alpha \le 1$ and consider two possibly correlated estimates for x, $(\hat{x}, P)$ and $(\hat{x}', P')$. Then the CI fusion algorithm yields

$$\begin{aligned} x^+ &= P^+\left(\alpha^* P^{-1}\hat{x} + (1-\alpha^*)P'^{-1}\hat{x}'\right) \\ &= \hat{x} - (1-\alpha^*)P^+P'^{-1}(\hat{x}-\hat{x}'), \\ P^+ &= \left(\alpha^* P^{-1} + (1-\alpha^*)P'^{-1}\right)^{-1}, \\ \alpha^* &= \operatorname*{argmin}_{0\le\alpha\le 1} \det\left(\alpha P^{-1} + (1-\alpha)P'^{-1}\right)^{-1}. \end{aligned} \tag{21}$$

Note that the second formula for x^+ given above is not standard and makes explicit how the prior estimate $\hat{x}$ is updated based on a new, possibly correlated estimate $\hat{x}'$. It is easy to check that the value for x^+ given by the CI algorithm (21) is the minimizer of the convex combination least squares cost

$$J(x) = \frac{\alpha^*}{2}\|x-\hat{x}\|^2_{P^{-1}} + \frac{(1-\alpha^*)}{2}\|x-\hat{x}'\|^2_{P'^{-1}}. \tag{22}$$

Therefore, we can introduce the following updated error energy measure for the true pose trajectory,

$$\begin{aligned} V^+(X,t) \coloneqq\ & \alpha_r^* V(X,t) \\ &+ \frac{(1-\alpha_r^*)}{2}\|\bar{y}(t) - X^{-1}(t)\bar{\hat{l}}\|^2_{\tilde{W}^{-1}}. \end{aligned} \tag{23}$$

Given a current estimate $(\hat{X}(t), P)$ of the true pose $X(t)$, current landmark estimate $(\hat{l}, P_l)$ and a landmark measurement $\bar{y}(t)$ of the landmark coordinates $\bar{l}$ obtained according to (12), the safe minimum-energy estimate $\hat{X}^+(t)$ minimizes the error energy cost (23). In other words, the task is to find

$$\hat{X}^+(t) \coloneqq \operatorname*{argmin}_X V^+(X,t)(t). \tag{24}$$

Denoting $\hat{\bar{y}} \coloneqq \hat{X}^{-1}\bar{\hat{l}}$, the resulting update step of the robot

pose filter is then [7, Eq. (38)]

$$\hat{X}^+ = \hat{X}\exp\left(\left(-(1-\alpha_r^*)P^+\begin{bmatrix}\hat{y}\times(W^{-1}(y-\hat{y}))\\ W^{-1}(y-\hat{y})\end{bmatrix}\right)^\wedge\right),$$
$$P^+ = \left(\alpha_r^* P^{-1} + (1-\alpha_r^*)Q\right)^{-1},\ Q \coloneqq \begin{bmatrix}Q_{11} & Q_{12}\\ Q_{12}^\top & Q_{22}\end{bmatrix},$$
$$Q_{11} \coloneqq \hat{y}_\times^\top W^{-1}\hat{y}_\times - \mathbb{P}_s((W^{-1}(y-\hat{y}))_\times \hat{y}_\times)), \tag{25}$$
$$Q_{12} \coloneqq \frac{1}{2}(W^{-1}(y-\hat{y}))_\times + \hat{y}_\times W^{-1},\ Q_{22} \coloneqq W^{-1}.$$

B. Landmark Estimation

The filter for the landmark position does not require a propagation step since the landmark is assumed to be stationary with respect to the global reference frame $\mathcal{A}$. Following the equivalent steps for the derivation of the update step of the filter as we did for the robot pose filter above yields the formulas

$$\begin{aligned} J(X,l) &= \frac{1}{2}\|\bar{y}(t) - X^{-1}(t)\bar{l}\|^2_{(\tilde{D}\tilde{D}^\top)^{-1}} \\ &\quad + \frac{1}{2}\|X(t)-\hat{X}(t)\|^2_{P(t)^{-1}}, \\ J^*(l) &= \frac{1}{2}\|\bar{y}(t) - \hat{X}^{-1}(t)\bar{l}\|^2_{\tilde{M}^{-1}}, \\ \tilde{M} &\triangleq \tilde{D}\tilde{D}^\top + H_X P H_X^\top, \\ H_X &= \begin{bmatrix}\left(\hat{R}^\top(\hat{l}-\hat{p})\right)_\times & -\hat{R}^\top \\ 0_{1\times 3} & 0_{1\times 3}\end{bmatrix} \end{aligned} \tag{26}$$

for the combination of the landmark measurement y with the current robot pose estimate $\hat{X}$. Next, we fuse this cost with the prior cost in a safe way

$$\begin{aligned} J^+(l) &= \frac{\alpha_l^*}{2}\|l-\hat{l}\|^2_{P_l^{-1}} \\ &\quad + \frac{(1-\alpha_l^*)}{2}\|y-\hat{R}^\top(l-\hat{p})\|^2_{M^{-1}}, \end{aligned} \tag{27}$$

which yields the following equations for the update step of the landmark position filter,

$$\begin{aligned} \hat{l}^+ &= \hat{l} + (1-\alpha_l^*)P_l^+\hat{R}M^{-1}\left(y-\hat{R}^\top(\hat{l}-\hat{p})\right), \\ P_l^+ &= \left(\alpha_l^* P_l^{-1} + (1-\alpha_l^*)\hat{R}M^{-1}\hat{R}^\top\right)^{-1}. \end{aligned} \tag{28}$$

V. Simulation Study

In this section, we provide a numerical example in order to demonstrate the performance of the proposed algorithm from Section IV. We will consider a unicycle robot that is localising its pose in the plane of operation using linear and angular velocity measurements and relative measurements with respect to four landmarks. While all landmarks are uniquely identifiable to the robot, the position of one of them with respect to the global reference frame $\mathcal{A}$ is unknown to the robot. The task is to localize the robot as well as this unknown landmark. We compare the performance of the proposed algorithm (labeled 'Safe' in this section), against an algorithm based on our previous work [16] for which we consider all four landmark positions to be known to the robot (labeled 'Baseline' in this section).

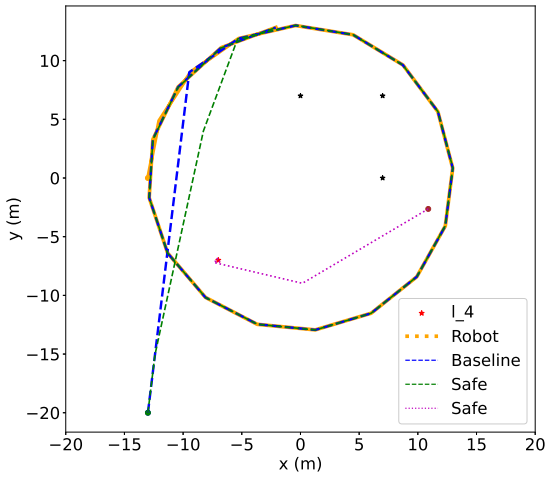

Fig. 2. Trajectory of the robot (Orange) and robot position estimate given by the proposed 'Safe' method (Green) and the 'Baseline' method (Blue), respectively. Only the 'Safe' method also estimates the position of landmark l_4 (Red), for which the estimation trajectory is shown in (Magenta). The circles indicate the initial estimates.

We implement the proposed equations using the unit quaternion representation of rotations. The first equation in (18) is geometrically integrated using the SE(3) exponential map in a first order Lie group Euler method. The Ricatti equation in (18) is numerically integrated using a first order Euler method. For more details we refer the reader to our previous work [12], [17]. The time step of the simulation is $dt = 1$. Angular and linear velocities $\Omega = [0, 0, -5/13]^\top$ and $V = [5, 0, 0]^\top$ are applied to the unicycle robot. These velocities are measured in the body-fixed frame $\mathcal{B}$ and are then used in the pose prediction equations (18). The velocities are measured according to (11) with $B_\omega = \pi/180 I\,(\frac{rad}{s})$ and $B_v = 0.1I\,(\frac{m}{s})$. We set $\delta_\omega = [0, 0, \delta_{\omega,z}]^\top, \delta_v = [\delta_{v,x}, 0, 0]$ where $\delta_{\omega,z}, \delta_{v,x} \sim \mathcal{N}(0,1)$ are random scalars drawn form the standard normal distribution $\mathcal{N}(0,1)$. The robot is initially at coordinates $p_r(0) = [-13, 0, 0]\,m$ with a random initial position estimate at $\hat{p}_r(0) = p_r(0) + [\delta_{r,x}, \delta_{r,y}, 0]\,m$ where $\delta_{r,x}, \delta_{r,y} \sim \mathcal{N}(0, 10)$. The initial attitude of the robot has zero roll and pitch but a yaw angle of $\pi/2$ (rad) while the initial estimate of the yaw angle is $95\pi/180$ (rad). The initial robot pose error covariance is $P(0) = \text{diag}([\pi/180, \pi/180, 25\pi/180, 100, 100, 1])$. Four landmarks are located at $l_1 = [0, 7, 0]^\top\,m$, $l_2 = [7, 0, 0]^\top\,m$, $l_3 = [7, 7, 0]^\top\,m$ and $l_4 = [-7, -7, 0]^\top\,m$ with respect to the global reference frame. The position of landmark l_4 is only known to the 'Baseline' algorithm. The 'Safe' algorithm has the initial estimate $\hat{l}_4 = l_4 + [\delta_{l,x}, \delta_{l,y}, 0]\,m$ where $\delta_{l,x}, \delta_{l,y} \sim \mathcal{N}(0, 10)$. The initial error covariance of the landmark position estimate $\hat{l}_4$ is $P_l(0) = \text{diag}([100, 100, 1])$.

The landmark measurements are simulated based on (12) with $\epsilon = [\epsilon_x, \epsilon_y, 0]^\top\,m$, $\epsilon_x, \epsilon_y \sim \mathcal{N}(0,1)$. The error coefficient matrix is set as $D = 0.01I\,m$.

Figure 2 on the previous page shows the trajectory of the robot conducting an orbiting maneuver around the four

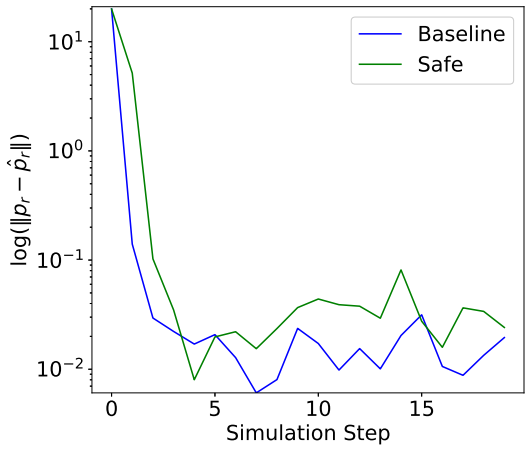

Fig. 3. Estimation error for robot position

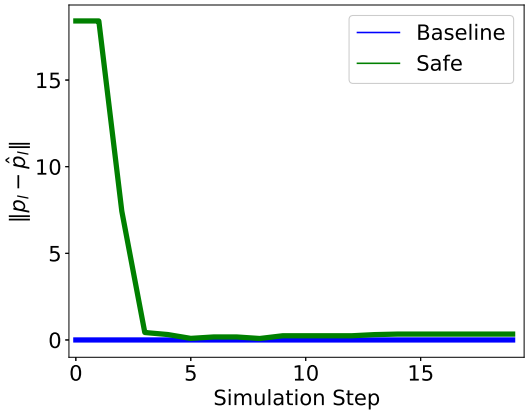

Fig. 4. Estimation error for the position of landmark l_4. The 'Baseline' method knows the position of l_4 perfectly while the proposed 'Safe' method estimates this.

landmarks as well as the robot position estimates produced by the two algorithms and the estimate $\hat{l}_4(t)$ produced by the 'Safe' algorithm. Figure 3 compares the robot position estimation errors incurred by the two methods demonstrating that the 'Safe' method achieves comparable performance to the 'Baseline' method despite not knowing the position of landmark l_4 in the global reference frame $\mathcal{A}$. For reference, Figure 4 shows the estimation error for the position of landmark l_4 incurred by the proposed 'Safe' method.

VI. Conclusion

We provide a modular nonlinear continuous-discrete Geometric Approximate Minimum Energy (GAME) filter for the problem of concurrent estimation of the 3D pose of a mobile robot and the 3D position of a landmark where reliable high rate velocity measurements are available but relative measurements of landmark positions are only available sporadically. The proposed algorithm incorporates a nonlinear version of Covariance Intersection (CI) to avoid double counting of information when the two filtering modules exchange correlated information in form of their respective state estimates and estimates of their error covariances. We demonstrate through numerical simulation that the proposed modular filter achieves comparable performance to a baseline filter that has access to the positions of all landmarks with respect to the global reference frame inviting further research to what extent this enables simple modular augmentation of existing filters for robotic applications to cover unexpected failure modes where, for example, the robot pose filter temporarily loses access to some of its measurement inputs.

References

[1] H. Durrant-Whyte and T. Bailey, "Simultaneous localization and mapping: part i," *IEEE robotics & automation magazine*, vol. 13, no. 2, pp. 99–110, 2006.

[2] K. Ebadi, L. Bernreiter, H. Biggie, G. Catt, Y. Chang, A. Chatterjee, C. E. Denniston, S.-P. Deschênes, K. Harlow, S. Khattak, *et al.*, "Present and future of slam in extreme environments: The darpa subt challenge," *IEEE Transactions on Robotics*, vol. 40, pp. 936–959, 2023.

[3] Y. Bar-Shalom, X. R. Li, and T. Kirubarajan, *Estimation with applications to tracking and navigation: theory algorithms and software*. John Wiley & Sons, 2004.

[4] S. I. Roumeliotis and G. A. Bekey, "Distributed multirobot localization," *IEEE Transactions on Robotics and Automation*, vol. 18, no. 5, pp. 781–795, 2002.

[5] S. M. Patole, M. Torlak, D. Wang, and M. Ali, "Automotive radars: A review of signal processing techniques," *IEEE Signal Processing Magazine*, vol. 34, no. 2, pp. 22–35, 2017.

[6] S. Park, S. Bokijonov, and Y. Choi, "Review of microsoft hololens applications over the past five years," *Applied sciences*, vol. 11, no. 16, p. 7259, 2021.

[7] B. Zamani and J. Trumpf, "Discrete update pose filter on the special euclidean group se (3)," in *2019 IEEE 58th Conference on Decision and Control (CDC)*. IEEE, 2019, pp. 635–641.

[8] A. Saccon, J. Trumpf, R. Mahony, and A. P. Aguiar, "Second-order-optimal filters on lie groups," in *52nd IEEE Conference on Decision and Control*. IEEE, 2013, pp. 4434–4441.

[9] J. K. Uhlmann, "Covariance consistency methods for fault-tolerant distributed data fusion," *Information Fusion*, vol. 4, no. 3, pp. 201–215, 2003.

[10] L. Chen, P. O. Arambel, and R. K. Mehra, "Estimation under unknown correlation: Covariance intersection revisited," *IEEE Transactions on Automatic Control*, vol. 47, no. 11, pp. 1879–1882, 2002.

[11] S. J. Julier and J. K. Uhlmann, "A non-divergent estimation algorithm in the presence of unknown correlations," in *Proceedings of the 1997 American Control Conference (Cat. No. 97CH36041)*, vol. 4. IEEE, 1997, pp. 2369–2373.

[12] M.-D. Hua, M. Zamani, J. Trumpf, R. Mahony, and T. Hamel, "Observer design on the special Euclidean group SE(3)," in *Proceedings of the 50th IEEE Conference on Decision and Control*, 2011, pp. 8169–8175.

[13] R. E. Mortensen, "Maximum-likelihood recursive nonlinear filtering," *Journal of Optimization Theory and Applications*, vol. 2, no. 6, pp. 386–394, 1968.

[14] L. Chen, P. O. Arambel, and R. K. Mehra, "Fusion under unknown correlation-covariance intersection as a special case," in *Proceedings of the Fifth International Conference on Information Fusion. FUSION 2002.(IEEE Cat. No. 02EX5997)*, vol. 2. IEEE, 2002, pp. 905–912.

[15] M. Reinhardt, B. Noack, P. Arambel, and U. Hanebeck, "Minimum covariance bounds for the fusion under unknown correlations," *IEEE Signal Processing Letters*, vol. 22, pp. 1210–1214, 2015.

[16] M. Zamani and A. P. Aguiar, "Distributed localization of heterogeneous agents with uncertain relative measurements and communications," in *Decision and Control (CDC), 2015 IEEE 54th Annual Conference on*. IEEE, 2015, pp. 4702–4707.

[17] M. Zamani, J. Trumpf, and R. Mahony, "Minimum-energy filtering for attitude estimation," *IEEE Transactions on Automatic Control*, vol. 58, no. 11, pp. 2917–2921, 2013.